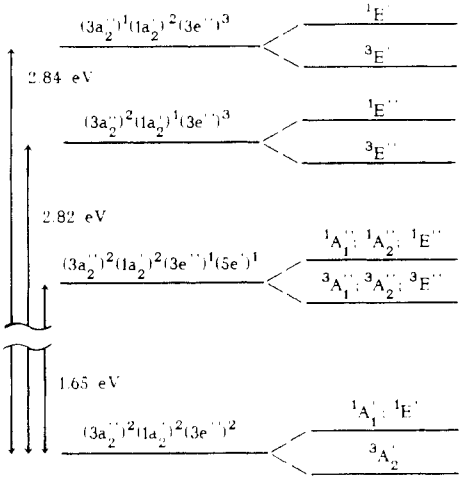


**Figure 4.** Plot of the ground state and some relevant excited states according to the MO calculation. The terms with the same spin multiplicity, which originate from one configuration, have been drawn schematically at the same level.

$^3A_2' \rightarrow {}^3E''$ ($1a_2' \rightarrow 3e''$) is electric dipole forbidden (Figure 4). If no corrections are made for electron–electron repulsion, then the calculated transition energies are given as above.

Although at 1.65 eV no band has been observed, the transition energy value of 2.84 eV is in rather good agreement with the observed value of 2.67 eV, in contrast to the value of 3.08 eV that has been found earlier with the more advanced HFS–DVM method,[5] starting from a tetrahedral environment. However, the possibility that the calculated 1.65-eV transition should be assigned to the observed band may not be excluded, as the accuracy of the Wolfsberg–Helmholz method is not very well established. Nevertheless, we assume that the lack of resemblance between calculated and observed spectra of ruthenate in the past was mainly due to the assumption of tetrahedral coordination for the ruthenium ion.

It may be very interesting to verify if the found coordination occurs in other ruthenates. Nowogrocki[9] et al. found certain similarities between $SrRuO_4 \cdot H_2O$ and $BaRuO_3(OH)_2$, and also the compound $NaRuO_4 \cdot H_2O$ would be a very interesting compound[3] to study.

For one perruthenate, $KRuO_4$, the structure was determined to be of the scheelite ($CaWO_4$) type.[20] However, this compound does not contain a $H_2O$ unit, and therefore $NaRuO_4 \cdot H_2O$ should not necessarily show the scheelite structure and thus is a probable candidate to exhibit the five-coordination. If this trigonal-bipyramidal configuration is found, the compound, containing a $d^1$ ion, might be subject to a Jahn–Teller distortion.

**Acknowledgment.** We wish to express our gratitude to Dr. R. A. G. De Graaff for his helpful suggestions during the crystal structure determination and to the first reviewer for his remark, leading to the selection of the correct enantiomorph. The investigations were supported in part (W.G.H.) by the Netherlands Foundation for Chemical Research (SON) with financial aid from the Netherlands Organization for the Advancement of Pure Research (ZWO).

**Registry No.** $K_2RuO_3(OH)_2$, 112113-56-1.

**Supplementary Material Available:** Table SI, listing the anisotropic thermal parameters, and Figures SI and SII, showing the coordination of the ruthenium and a projection of the structure on the *ab* plane, respectively (3 pages); Table SII, listing the observed and calculated structure factors (12 pages). Ordering information is given on any current masthead page.

---

Contribution from the Department of Chemistry and Chemical Physics Program, Washington State University, Pullman, Washington 99163, and Gorlaeus Laboratories, Leiden University, P.O. Box 9502, 2300 RA Leiden, The Netherlands

# Crystal Structures of Three Phases of Tetramethylammonium Trichlorocuprate(II) (TMCuC)

Roger D. Willett,*† Marcus R. Bond,† W. G. Haije,‡ O. P. M. Soonieus,‡ and W. J. A. Maaskant‡

*Received May 1, 1987*

The compound tetramethylammonium trichlorocuprate(II), $C_4H_{12}NCuCl_3$, exhibits two crystalline phase transitions, one at 319 K and the other at 373 K. X-ray structure determinations of the three corresponding phases were carried out at 213.2 (3), 323 (2), and 405 (2) K. These structures are deformed members of the hexagonal perovskite family (2L): crystal data at 213 K, monoclinic $P2_1$, $a$ = 8.948 (8) Å, $b$ = 32.225 (10) Å, $c$ = 8.980 (2) Å, $\beta$ = 119.487 (18)°; crystal data at 323 K, triclinic $P\bar{1}$, $a$ = 9.082 (5) Å, $b$ = 9.073 (5) Å, $c$ = 6.442 (3) Å, $\alpha$ = 90.05 (4)°, $\beta$ = 92.40 (4)°, $\gamma$ = 119.99 (3)°; crystal data at 405 K, hexagonal $P6_3/mmc$, $a = b$ = 9.160 (2) Å, $c$ = 6.474 (2) Å. In the high-temperature phase (2L) the Jahn–Teller elongation is disordered over three possible configurations, $x$, $y$, and $z$, in the intermediate-temperature phase (2L) one site is ordered ($z$) and the other is disordered over two configurations ($x$ and $y$), and the low-temperature phase (10L) exhibits a static structure as far as the Jahn–Teller effect is concerned. All phases show disorder of the tetramethylammonium group except for the low-temperature phase, which is partially ordered with respect to this ion. This means that there must be another phase at lower temperature.

## Introduction

One class of structural types exhibited by $ACuCl_3$ salts (A = monopositive cation)[1] is a Jahn–Teller-distorted version of the $CsNiCl_3$ structure.[2] The latter contains parallel chains of face-sharing $NiCl_6$ octahedra separated by the Cs cations (see Figure 1). In the copper(II) salts, the octahedra assume a tetragonally elongated 4 + 2 coordination geometry such that each $Cu^{2+}$ ion has four short (~2.3-Å) and two long (2.8–3.2-Å) Cu–Cl bonds. The neighboring $Cu^{2+}$ ions are linked by one symmetrical Cu–Cl–Cu bridge (both Cu–Cl bonds ~2.3 Å) and two asymmetrical bridges involving one short and one long Cu–Cl bond. Cu–Cl–Cu bridges involving two long Cu–Cl bonds are energetically unfavorable and have not been observed experimentally. This introduces a cooperative nature into the Jahn–Teller distortions within the chain structure whereas the cooperative nature between the chains originates from the elastic interactions via the close-packed Cl layers. Any individual $CuCl_6$ octahedron can undergo a Jahn–Teller elongation along one of its three "4-fold" axes; however, the distortion assumed by this octahedron is now

† Washington State University.
‡ Leiden University.

(1) Willett, R. D.; Geiser, U. *Croat. Chem. Acta* **1984**, *57*, 737.
(2) Tishchenko, G. N. *Tr. Inst. Kristallogr., Akad. Nauk SSSR* **1955**, *11*, 93; *Gmelins Handbuch der Anorganischen Chemie*, 8th ed.; Springer-Verlag: New York, 1966; Nickel Compounds B-3, p 1103.

 

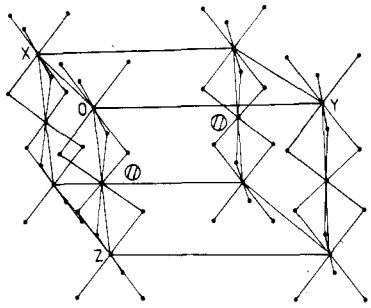


**Figure 1.** Unit cell diagram of a hypothetical undistorted $(CH_3)_4NCuCl_3$ structure. The cations are at the positions of the hatched circles.

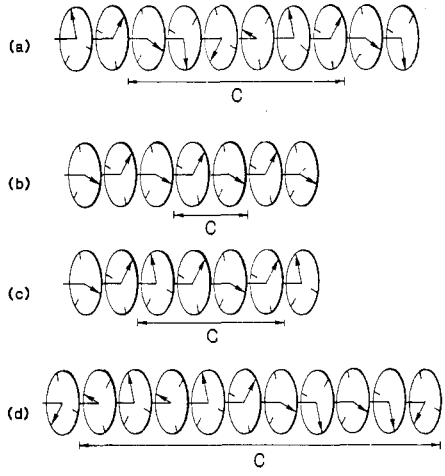


**Figure 2.** Schematic representation of the direction of the Jahn–Teller distortion in several tribridged-chain structures. C denotes the repeat distance along the chains (a) $CsCuCl_3$, (b) high-temperature $(CH_3)_2CHNH_3CuCl_3$, (c) low-temperature $RbCuCl_3$ (presumed), and (d) TMCuC.

restricted by the orientation of the distortion assumed by its neighbors.

This cooperativity is revealed in the crystal structures of the various $ACuCl_3$ salts containing tribridged chains. It is possible to characterize the nature of the cooperativity in the following manner. For each $Cu^{2+}$ ion, the Jahn–Teller-elongated Cu–Cl bond pointing in the "up" direction is projected onto a plane normal to the chain direction. As one progresses up the chain, these projected vectors may undergo rotations of ±60°. (Rotation by 180° corresponds to two long Cu–Cl bonds to the same bridging chloride ion and thus is not allowed.) The system thus maps onto the one-dimensional spin-$^1/_2$ Ising model.[3] The observed structures then correspond to various repeated patterns of ±60° rotations and are illustrated schematically in Figure 2. In $CsCuCl_3$, a helical structure is found,[4] in which each successive rotation has the same sense, e.g., always +60° (Figure 2a). The high-temperature phase of $(CH_3)_2CHNH_3CuCl_3$[5] has the pattern in Figure 2b, in which the repeating sequence is (+60, −60°). In the language associated with magnetic systems, these structures correspond to ferromagnetic and antiferromagnetic ordering, respectively. The low-temperature phase of $RbCuCl_3$ is described by a (+60, +60, −60, −60°) pattern as in Figure 2c.[6] Finally, the low-temperature structure of $(CH_3)_4NCuCl_3$ (TMCuC) exhibits the rather unusual pattern in Figure 2d,[7] in which the repeat unit involves a (+60, +60, +60, +60, −60°) sequence. Both

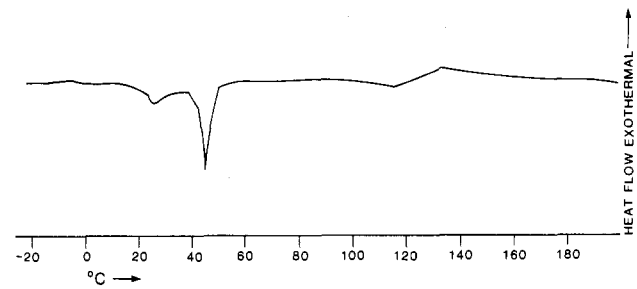


**Figure 3.** DSC curve showing the phase transition at 319 K (probably of first order) and 373 K (probably of second order).

$CsCuCl_3$[8] and $RbCuCl_3$[6] undergo transitions to disordered (paradistortive) phases at higher temperatures.

In this paper we report on studies of three phases of TMCuC, including both DSC and crystallographic studies. The DSC studies indicate phase transitions at 319 and 373 K. The crystal structures of the low-, intermediate-, and high-temperature phases will be presented. These structures will be discussed in relation to both the Jahn–Teller effect and strain.

## Experimental Section

**Synthesis.** Red, needle-shaped crystals were grown from a saturated aqueous solution containing stoichiometric amounts of $CuCl_2 \cdot 2H_2O$ and $(CH_3)_4NCl$ ((TMA)Cl) and an excess of HCl. The crystallization of the low-temperature form was carried out at room temperature over $P_2O_5$ in a desiccator. The crystals used for the measurements above 319 K were grown at 323 K. This last step was necessary since previous X-ray work showed that single crystallinity was lost upon heating the crystal above the transition temperature. On examination it was found that all crystals of appreciable size grown at 323 K were multiply twinned with each single diffraction spot being replaced by a pattern of six spots, the twinning presumably occurring about the vertical mirror planes in the high-temperature hexagonal phase. A contrasting feature is shown by crystals grown at room temperature and heated above the first transition temperature. These show all characteristics of rotation twinning[9] around the $c$ axis of the centered space group $B\bar{1}$ where the $b$ axis is the original hexagonal axis (the coordinate system is right-handed).

**DSC Studies.** The DSC measurements were carried out on a Mettler TA3000 system between 103 and 473 K. Reliable detection of the signal occurs above 133 K. The scan reveals two distinct transitions, one at 319 K being probably of first order and one starting at about 373 K but being less well-defined presumably due to a second-order transition. Other irregularities in the base line have not yet been identified as having any physical meaning (Figure 3).

**Crystal Structure Determinations. Low-Temperature (213 K) Phase.** The crystal structure at room temperature of this phase has been determined previously by Weenk and Spek.[7] Their structure refinement resulted in an $R_w$ value equal to 14%. This leads to a fairly accurate description of the $CuCl_3$ chain but left the TMA cations ill-defined. As the large thermal motion obscured a good description of the structure, a new X-ray data collection was carried out at lower temperature. A single crystal of dimensions 0.50 mm × 0.26 mm × 0.22 mm was mounted on an Enraf-Nonius CAD4 diffractometer equipped with a cooling stage. The $N_2$ gas stream was held at a temperature of −60.0 (3)° C. Determination of the lattice constants using 24 reflections yielded a monoclinic lattice with $a$ = 8.948 (8) Å, $b$ = 32.225 (10) Å, $c$ = 8.980 (2) Å, $\beta$ = 119.487 (18)°, $V$ = 2254.21 (2) Å$^3$, and $\rho$ = 1.80 g/cm$^3$ ($Z$ = 10). Data collection conditions and parameters are summarized in Table I. No absorption correction was applied. The data were corrected for decay of the scattering power and Lp effects. Scattering factors were taken from ref 10 with correction for the real and imaginary part of the anomalous dispersion. The measured intensities of symmetry-related reflections were averaged. The function minimized during the least-squares refinement was $\sum w(|F_o| - |F_c|)^2$, $w = 1/\sigma(F)^2$, where $\sigma(F)$ is the esd calculated from counting statistics and errors in

(3) Tanaka, H.; Dachs, H.; Iio, K.; Nagata, K. *J. Phys. C* **1986**, *19*, 4861, 4879.
(4) Wells, A. F. *J. Chem. Soc.* **1947**, 1662. Schlueter, A. W.; Jacobson, R. A.; Rundle, R. E. *Inorg. Chem.* **1966**, *5*, 277.
(5) Roberts, S. A.; Bloomquist, D. R.; Willett, R. D.; Dodgen, H. W. *J. Am. Chem. Soc.* **1981**, *103*, 2603.
(6) Crama, W. J. Ph.D. Thesis, Rijksuniversiteit Leiden, Leiden, The Netherlands, 1980. Harada, M. *J. Phys. Soc. Jpn.* **1982**, *51*, 2053; **1983**, *52*, 1646.
(7) Weenk, J. W.; Spek, A. L. *Cryst. Struct. Commun.* **1976**, *5*, 805.
(8) Kroese, C. J.; Tindemans-van Eyndhoven, J. C. M.; Maaskant, W. J. A. *Solid State Commun.* **1971**, *9*, 1707. Kroese, C. J.; Maaskant, W. J. A.; Verschoor, G. C. *Acta Crystallogr., Sect. B: Struct. Crystallogr. Cryst. Chem.* **1974**, *B30*, 1053.
(9) Boulesteix, C.; van Landuyt, J.; Amelinckx, S. *Phys. Status Solidi A* **1976**, *33*, 595.
(10) *International Tables for X-ray Crystallography*; Kynoch: Birmingham, England, 1974; Vol. IV (present distributor D. Reidel, Dordrecht, The Netherlands).

**Table I.** TMCuC Structure Determination Data

| | 213 K | 323 K | 405 K |
|---|---|---|---|
| empirical formula | | $C_4H_{12}NCuCl_3$ | |
| mol wt | | 244.05 | |
| cryst class | monoclinic | triclinic | hexagonal |
| space group | $P2_1$ | $P\bar{1}$ | $P6_3/mmc$ |
| systematic absences | $0k0$, $k$ odd | none | $h,h,2\bar{h},l$, $l$ odd |
| lattice constants | | | |
| $a$, Å | 8.948 (8) | 9.082 (5) | 9.160 (2) |
| $b$, Å | 32.225 (10) | 9.073 (5) | 9.160 (2) |
| $c$, Å | 8.980 (2) | 6.442 (3) | 6.474 (2) |
| $\alpha$, deg | 90 | 90.05 (4) | 90 |
| $\beta$, deg | 119.487 (18) | 92.40 (4) | 90 |
| $\gamma$, deg | 90 | 119.99 (3) | 120 |
| vol, Å$^3$ | 2254.21 (2) | 459.2 (4) | 470.4 (3) |
| cryst size, mm | 0.50 × 0.26 × 0.22 | 0.16 × 0.16 × 0.40 | 0.29 × 0.35 × 0.52 |
| calcd density, $\rho$, g/cm$^3$ | 1.80 | 1.77 | 1.72 |
| $Z$ | 10 | 2 | 2 |
| $\mu$, cm$^{-1}$ | 31.75 | 31.93 | 31.17 |
| diffractometer syst | CAD4 | Nicolet R3m/E | upgraded Syntex $P2_1$ |
| radiation | | Mo K$\alpha$ with graphite monochromator ($\lambda$ = 0.710 69 Å) | |
| data collecn method | bisect (zigzag) | $\omega$ scans | $\omega$ scans |
| scan range, deg | 1.19 | 1.2 | 1.1 |
| scan speed, deg/min | | 4.0–29.3 | |
| check reflns | $\bar{6}65$; $\bar{5}80$; 085; $0,\bar{2}2,0$ | $\bar{1}\bar{1}2$; $3\bar{3}2$ | $\bar{5}30$; $0\bar{2}\bar{1}$; $\bar{2}2\bar{1}$ |
| abs cor | none | empirical | numerical |
| transmission factors | | 0.60 (max), 0.48 (min) | 0.42 (max), 0.24 (min) |
| $E$(000) | 1230 | 246 | 246 |
| total no. of reflns | 7065 | 1842 | 1753 |
| $2\theta$(max), deg | 60 | 49 | 50 |
| no. of unique reflns | 6694 | 1596 | 182 |
| no. of obsd reflns | 4929 | 1220 | 178 |
| soln technique | | direct methods | |
| $R$ | 0.0498 | 0.0754 | 0.0628 |
| $R_w$ | 0.0594[a] | 0.0851[b] | 0.0604[b] |
| $\Delta/\sigma$(mean) | 0.000 | 0.004 | 0.000 |
| $\Delta/\sigma$(max) | 0.01 | 0.016 | 0.001 |
| total no. of params refined | 361 | 143 | 25 |
| thermal params | anisotropic on non-C | anisotropic on non-H | anisotropic on non-C |
| H atoms | not calcd | constrained to C–H = 0.96 Å | not calcd |
| extinction cor | | none | |

[a] The function minimized was $\sum w(|F_o| - |F_c|)^2$, $w = 1/\sigma(F)^2$. [b] The function minimized was $\sum w(|F_o| - |F_c|)^2$, $w = [\sigma(F)^2 + gF^2]^{-1}$; $g$ = 0.001 49 for 323 K and 0 for 405 K (refined values).

the aforementioned corrections. For all calculations computer programs written or modified by Rutten-Keulemans and De Graaff were used on the Leiden University Amdahl V7B computer. The positions of the Cu and Cl ions were determined from direct methods. Difference Fourier techniques supplied the positional parameters of the N and C atoms. A least-squares refinement of a model including anisotropic thermal parameters for the carbon atoms resulted in an $R_w$ value of 0.0585. Some of the $NC_4$ tetrahedra showed very large anisotropies for the C atoms. The directions of these anisotropies suggested large-amplitude thermal motion (libration) of the tetrahedron around a particular axis. A model was refined in which the C positions were split up in a way consistent with the direction of the thermal motion, and both positions were given an occupancy of 0.5. The refinement was carried out with isotropic thermal parameters for the disordered C's, as anisotropic parameters gave rise to nonpositive-definite temperature factors. Furthermore, the C–N and C–C distances within those tetrahedra were constrained to 1.50 (2) and 2.45 (3) Å, respectively. The resulting $R_w$ value amounted to 0.060. Eventually the positions of 10 H atoms could be identified, which lowered the $R_w$ to 0.059. This $R$ value is very close to the purely anisotropic result. The physical picture of the disordered model, however, better illustrates the difference between the two different kinds of TMA cations, the static ones and the librating ones. The coordinates and equivalent isotropic parameters of the non-hydrogen atoms can be found in Table II. Tables of anisotropic thermal parameters, hydrogen atom coordinates, and observed and calculated structure factors are reported in the supplementary material.

**Intermediate-Temperature (323 K) Phase.** After careful examination, a single crystal of TMCuC (intermediate-temperature phase) was mounted and placed on a Nicolet R3m/E diffractometer. A heater mounted independently of the diffractometer was placed such that a stream of heated air impinged on the crystal. The temperature of the gas stream was controlled via a feedback circuit connected to an iron–constantan thermocouple placed in the gas stream. In addition the temperature at the center of the diffractometer circle was calibrated with an iron–constantan thermocouple. The temperature was measured as 323 (2) K at the center prior to mounting the crystal. A least-squares refinement of the angular settings of 25 well-centered reflections with $2\theta$ between 29 and 31° yielded triclinic lattice constants $a$ = 9.082 (5) Å, $b$ = 9.073 (5) Å, $c$ = 6.442 (3) Å, $\alpha$ = 90.05 (4)°, $\beta$ = 92.40 (4)°, $\gamma$ = 119.99 (3)°, $V$ = 459.2 (4) Å$^3$, and a calculated density of 1.77 g/cm$^3$ ($Z$ = 2). Data were collected[11] in the $h > 0$, all $k$, all $l$ hemisphere of reciprocal space. Data collection conditions and parameters are summarized in Table I. Two reflections were rejected because of asymmetric peak shapes, and 19 were rejected because of background imbalance. An empirical absorption correction, assuming an ellipsoidal crystal shape, was performed on the data. Lp corrections and a crystal decay correction, derived from a curve fitted to the intensities of standards during the data collection, were applied to the data. Equivalent reflection intensities were averaged together by using the MERG command in SHELXTL ($R_{merg}$ = 0.0724). The structure was solved and refined with the SHELXTL[12] package of programs provided by Nicolet. The space group $P\bar{1}$ was chosen for initial refinement. The positions of the copper and chlorine ions were identified from the $E$ map calculated from direct methods. Refinement of these atom positions using a blocked-cascade least-squares method with isotropic thermal parameters and unit weights yielded $R$ = 0.2171. Addition of anisotropic thermal parameters lowered $R$ to 0.1688. Addition of nitrogen and four carbon atom positions identified from the electron density difference map gave a value of $R$ = 0.1032 for the refinement. Since the $U_{33}$ values for Cl(2) and Cl(3) were abnormally large, disorder of the two atoms was assumed and positions 0.2 Å apart on $z$ were added to the refinement to give $R$ = 0.0944. Refinement of the site occupation factors yielded 0.460 (4) for the pair Cl(2a), Cl(3) and 0.540 (4) for the pair Cl(2), Cl(3a). Analysis of the electron density difference map showed four more carbon positions, indicating disorder

(11) Campana, C. F.; Shepard, D. F.; Litchman, W. M. *Inorg. Chem.* **1981**, *20*, 4039.
(12) Sheldrick, G. M. *SHELXTL, Revision 4.1*; Nicolet Instrument Corp.: Madison, WI, 1985. Scattering factors are from ref 10.

**Table II.** Positional Parameters and Equivalent Isotropic $B$ Values of TMCuC at 213 K[a]

| atom | $x/a$ | $y/b$ | $z/c$ | $B_{iso}$, Å$^2$ | atom | $x/a$ | $y/b$ | $z/c$ | $B_{iso}$, Å$^2$ |
|---|---|---|---|---|---|---|---|---|---|
| Cu(1) | −141 (2) | 1077 (0) | 316 (1) | 171 (2) | C(12a) | −493 (1) | 64 (1) | 415 (2) | 24 (2) |
| Cu(2) | −237 (2) | 2106 (0) | 84 (1) | 170 (3) | C(13a) | −246 (2) | 19 (0) | 470 (2) | 33 (3) |
| Cu(3) | −814 (2) | 3121 (0) | −82 (1) | 162 (3) | C(14a) | −220 (2) | 95 (0) | 474 (2) | 41 (3) |
| Cu(4) | −838 (1) | 4096 (0) | −878 (1) | 166 (3) | C(11b) | −401 (2) | 44 (1) | 202 (1) | 33 (3) |
| Cu(5) | −60 (2) | 5069 (0) | −855 (1) | 157 (3) | C(12b) | −492 (1) | 55 (1) | 414 (2) | 24 (2) |
| Cl(1) | −2634 (3) | 716 (1) | −1078 (3) | 225 (6) | C(13b) | −197 (2) | 30 (0) | 503 (2) | 33 (3) |
| Cl(2) | 837 (3) | 507 (1) | 3106 (3) | 208 (6) | C(14b) | −275 (2) | 103 (0) | 413 (2) | 41 (3) |
| Cl(3) | 1175 (3) | 527 (1) | −362 (3) | 201 (6) | C(21a) | 444 (1) | 156 (1) | −370 (2) | 42 (3) |
| Cl(4) | −1437 (3) | 1605 (1) | 1080 (3) | 234 (6) | C(22a) | 133 (2) | 161 (1) | −468 (2) | 37 (3) |
| Cl(5) | 2343 (3) | 1445 (1) | 1504 (3) | 254 (6) | C(23a) | 341 (2) | 127 (1) | −184 (2) | 52 (4) |
| Cl(6) | −1144 (3) | 1735 (1) | −2364 (3) | 233 (6) | C(24a) | 325 (2) | 202 (0) | −228 (2) | 45 (4) |
| Cl(7) | 479 (3) | 2670 (1) | −1135 (3) | 222 (6) | C(21b) | 444 (1) | 167 (1) | −371 (2) | 42 (3) |
| Cl(8) | −3059 (3) | 2678 (1) | −898 (3) | 218 (6) | C(22b) | 148 (2) | 144 (1) | −451 (2) | 37 (3) |
| Cl(9) | 1100 (3) | 2452 (1) | 2612 (3) | 234 (6) | C(23b) | 398 (2) | 142 (1) | −139 (2) | 52 (4) |
| Cl(10) | 1353 (3) | 3614 (1) | 512 (3) | 184 (5) | C(24b) | 254 (2) | 205 (0) | −295 (2) | 45 (4) |
| Cl(11) | −2237 (3) | 3628 (1) | −3024 (3) | 209 (6) | C(31a) | −392 (2) | 257 (1) | 499 (1) | 28 (2) |
| Cl(12) | −1738 (3) | 3544 (1) | 1333 (3) | 215 (6) | C(32a) | −193 (1) | 259 (1) | 388 (2) | 28 (3) |
| Cl(13) | −3014 (3) | 4558 (1) | −2288 (3) | 217 (6) | C(33a) | −463 (2) | 220 (0) | 232 (2) | 40 (3) |
| Cl(14) | 1337 (3) | 4632 (1) | −1760 (3) | 216 (6) | C(34a) | −461 (2) | 298 (0) | 248 (2) | 35 (3) |
| Cl(15) | 521 (3) | 4582 (1) | 1321 (3) | 189 (5) | C(31b) | −423 (2) | 254 (1) | 480 (1) | 28 (2) |
| N(1) | −341 (1) | 58 (0) | 385 (1) | 19 (2) | C(32b) | −196 (1) | 272 (1) | 415 (2) | 28 (3) |
| N(2) | 311 (1) | 161 (0) | −312 (1) | 22 (2) | C(33b) | −398 (2) | 215 (0) | 259 (2) | 40 (3) |
| N(3) | −378 (1) | 258 (0) | 340 (1) | 19 (2) | C(34b) | −492 (2) | 289 (0) | 209 (2) | 35 (3) |
| N(4) | 271 (1) | 362 (0) | −375 (1) | 19 (2) | H(411) | 115 (1) | 379 (0) | −289 (2) | 57 (2) |
| N(5) | −372 (1) | 456 (0) | 267 (1) | 18 (2) | H(412) | 28 (1) | 359 (0) | 491 (2) | 57 (2) |
| C(41) | 100 (1) | 354 (0) | −384 (2) | 39 (4) | H(421) | −452 (1) | 352 (0) | −134 (1) | 64 (2) |
| C(42) | 407 (1) | 366 (0) | −191 (1) | 31 (3) | H(422) | 380 (1) | 390 (0) | −152 (1) | 64 (2) |
| C(43) | 256 (2) | 401 (0) | −474 (2) | 43 (4) | H(431) | 623 (2) | −85 (0) | 459 (2) | 56 (1) |
| C(44) | 319 (2) | 327 (0) | −455 (2) | 51 (5) | H(432) | −225 (2) | −79 (0) | 410 (2) | 56 (1) |
| C(51) | −472 (2) | 417 (0) | 254 (2) | 45 (4) | H(433) | 125 (2) | 398 (0) | 379 (2) | 56 (1) |
| C(52) | −381 (2) | 462 (0) | 98 (2) | 40 (4) | H(441) | 279 (2) | 307 (0) | −404 (2) | 18 (1) |
| C(53) | −184 (1) | 450 (0) | 403 (2) | 38 (3) | H(442) | 235 (2) | 325 (0) | 400 (2) | 18 (1) |
| C(54) | −452 (2) | 490 (0) | 310 (2) | 52 (5) | H(443) | −547 (2) | 338 (0) | −429 (2) | 18 (1) |
| C(11a) | −404 (2) | 57 (1) | 197 (1) | 33 (3) | | | | | |

[a] Positional parameters are ×10$^4$ for Cu and Cl and ×10$^3$ for all other atoms; $B_{iso}$ values are ×10$^5$ for Cu and Cl, ×10$^3$ for N, C(41)–C(44), and C(51)–C(55), and ×10 for all other atoms. Estimated standard deviations in the least significant digits are given in parentheses.

of the tetramethylammonium ion. Hydrogen atom positions were calculated and fixed such that the C–H bond distance was 0.96 Å and the hydrogen atoms were staggered with respect to the other carbon atoms. Anisotropic thermal parameters were refined for all non-hydrogen atoms, while a common isotropic thermal parameter was refined for the hydrogen atoms. C–N bond lengths were loosely constrained to a common refined value of 1.434 (9) Å, and C–C distances in a given orientation were loosely constrained to 1.633 times the average C–N bond length. Refined fractional occupancies for the two tetramethylammonium ion configurations yielded 0.55 (2) for one and 0.45 (2) for the other (the "a" configuration). Coordinates of non-hydrogen atoms with equivalent isotropic thermal parameters are found in Table III, while tables of anisotropic thermal parameters for these atoms, hydrogen atom coordinates, and observed and calculated structure factors are reported in the supplementary material. Refinement of this model in the space group $P1$ gave $R_w$ = 0.0773 with 272 least-squares parameters. The Hamilton test was not performed because the noncentrosymmetric structure is severely underdetermined. The fact that fewer parameters are involved in the centrosymmetric space group justifies the choice for it. The largest peak on the final electron-density difference map was found near (1.01 Å from) Cu(2), with a magnitude of 1.6 e/Å$^3$.

**High-Temperature (405 K) Phase.** A larger crystal of TMCuC (intermediate-temperature phase) was mounted on a glass fiber and placed on a Syntex $P2_1$ automated four-circle diffractometer upgraded to Nicolet R3m specifications. The crystal temperature was controlled by the same apparatus as described in the previous section. A rotation photograph at ~323 K showed the crystal to be multiply twinned; however, a rotation photograph taken at 405 (2) K revealed loss of the twinning. Least-squares refinement of the angular settings of 25 well-centered reflections between 22 and 35° on $2\theta$ yielded hexagonal unit cell constants of $a = b = 9.160$ (2) Å, $c = 6.474$ (2) Å, $V = 470.4$ (3) Å$^3$, and $\rho = 1.72$ g/cm$^3$ ($Z = 2$). Data were collected[11] in the $h > 0$, all $k$, all $l$ hemisphere of reciprocal space. Data collection conditions and parameters are summarized in Table I. Lp corrections and a crystal decay correction derived from a curve fitted to the intensities of the standards during the data collection were applied to the data. Equivalent reflections were averaged together under the MERG command in SHELXTL ($R_{merg}$ = 0.0541). A numerical absorption correction was applied prior to merging the equivalent reflections. The Nicolet SHELXTL[12] package of programs was used in solving and refining the structure. Examination of the data showed that reflections with indices $h,h,2\bar{h},l$, $l$ odd, were systematically absent, designating the space group as $P6_3/mmc$, $P\bar{6}2c$, or $P6_3mc$. The centrosymmetric space group was chosen for initial refinement. The copper, chlorine, and nitrogen atoms were identified from the $E$ map calculated from direct methods. Refinement of these atom positions with anisotropic thermal parameters and unit weights gave $R$ = 0.1143. An anomalously large thermal parameter on the chloride ion and the appearance of a large peak on the electron density difference map near the chloride ion indicated disorder of the ion. The chloride ion was then disordered over three possible sites with the occupancy factor of each site fixed at $^1/_3$. One of the carbon atom positions was identified from a subsequent electron density difference map; however, the other carbon

**Table III.** Atomic Coordinates and Isotropic Thermal Parameters for the TMCuC Intermediate-Temperature Phase[a]

| | $x$ | $y$ | $z$ | $U$,[b] Å$^2$ |
|---|---|---|---|---|
| Cu(1) | 0 | 0 | 0 | 55 (1)* |
| Cu(2) | 0 | 0 | 5000 | 60 (1)* |
| Cl(1) | 2445 (3) | 1219 (4) | 2079 (4) | 88 (1)* |
| Cl(2a) | −1101 (6) | −2179 (7) | 2409 (8) | 85 (2)* |
| Cl(3a) | −1104 (8) | 1099 (8) | 2306 (9) | 90 (3)* |
| Cl(2) | −1280 (7) | −2585 (6) | 3077 (7) | 69 (2)* |
| Cl(3) | −1246 (6) | 1284 (6) | 3024 (7) | 78 (2)* |
| N | −3343 (7) | −6664 (7) | 7500 (9) | 47 (3)* |
| C(1) | −404 (4) | −571 (4) | 845 (6) | 17 (3)* |
| C(2) | −410 (4) | −833 (3) | 841 (6) | 17 (3)* |
| C(3) | −371 (6) | −683 (6) | 533 (3) | 37 (5)* |
| C(4) | −154 (2) | −580 (6) | 796 (7) | 18 (2)* |
| C(1a) | −306 (5) | −651 (6) | 970 (3) | 27 (4)* |
| C(2a) | −428 (4) | −841 (2) | 687 (7) | 14 (2)* |
| C(3a) | −433 (4) | −588 (4) | 687 (7) | 13 (2)* |
| C(4a) | −176 (3) | −585 (5) | 652 (6) | 20 (4)* |

[a] Atomic coordinates are ×10$^4$ for Cu, Cl, and N and ×10$^3$ for C; thermal parameters are ×10$^3$ for Cu, Cl, and N and ×10$^2$ for C. [b] The equivalent isotropic $U$ (denoted by an asterisk) is defined as one-third of the trace of the orthogonalized $U_{ij}$ tensor.

**Table IV.** Atomic Coordinates and Isotropic Thermal Parameters for the TMCuC High-Temperature Phase[a]

| | x | y | z | U,[b] Å² |
|---|---|---|---|---|
| Cu | 0 | 0 | 0 | 79 (1)* |
| Cl | 2041 (20) | 1021 (10) | 2500 | 73 (6)* |
| Cl(1) | 2577 (10) | 1289 (5) | 3093 (17) | 85 (4)* |
| N | 3333 | 6667 | 2500 | 67 (4)* |
| C(1) | 428 (2) | 857 (4) | 250 | 11 (1) |
| C(2) | 296 (2) | 591 (5) | 41 (6) | 15 (2) |
| C(3) | 453 (3) | 617 (4) | 363 (3) | 10 (1) |

[a] See footnote *a* of Table III. [b] See footnote *b* of Table III.

**Table V.** Relevant Distances (Å) in the $CuCl_3$ Chain of the Low-Temperature Phase

| | | | |
|---|---|---|---|
| Cu(1)–Cu(2) | 3.322 (2) | Cu(2)–Cu(3) | 3.303 (2) |
| Cu(3)–Cu(4) | 3.221 (2) | Cu(4)–Cu(5) | 3.207 (2) |
| Cu(5)–Cu(1′) | 3.276 (2) | Cu(1)–Cl(1) | 2.267 (3) |
| Cu(1)–Cl(2) | 2.876 (3) | Cu(1)–Cl(3) | 2.364 (3) |
| Cu(1)–Cl(4) | 2.348 (3) | Cu(1)–Cl(5) | 2.271 (3) |
| Cu(1)–Cl(6) | 2.993 (3) | Cu(2)–Cl(4) | 2.345 (3) |
| Cu(2)–Cl(5) | 2.932 (3) | Cu(2)–Cl(6) | 2.272 (3) |
| Cu(2)–Cl(7) | 2.368 (3) | Cu(2)–Cl(8) | 2.891 (3) |
| Cu(2)–Cl(9) | 2.271 (3) | Cu(3)–Cl(7) | 2.328 (3) |
| Cu(3)–Cl(8) | 2.272 (3) | Cu(3)–Cl(9) | 3.057 (3) |
| Cu(3)–Cl(10) | 2.355 (3) | Cu(3)–Cl(11) | 2.822 (3) |
| Cu(3)–Cl(12) | 2.279 (3) | Cu(4)–Cl(10) | 2.326 (3) |
| Cu(4)–Cl(11) | 2.276 (3) | Cu(4)–Cl(12) | 3.056 (3) |
| Cu(4)–Cl(13) | 2.276 (3) | Cu(4)–Cl(14) | 2.986 (3) |
| Cu(4)–Cl(15) | 2.337 (3) | Cu(5)–Cl(13) | 2.828 (3) |
| Cu(5)–Cl(14) | 2.280 (3) | Cu(5)–Cl(15) | 2.356 (3) |
| Cu(5)–Cl(1′) | 3.009 (3) | Cu(5)–Cl(2′) | 2.277 (3) |
| Cu(5)–Cl(3′) | 2.334 (3) | | |

atoms could not be identified due to the extreme disorder of the tetramethylammonium ion and reasonable positions were calculated for refinement. The C–N bond lengths were loosely constrained to a common refined length of 1.52 (2) Å with the C–C distance within a given orientation of the TMA ion loosely constrained to 1.633 times the average C–N bond length. No hydrogen positions were calculated because of the extreme disorder of the tetramethylammonium ion. The final refinement of the structure gave $R = 0.0628$ and $R_w = 0.0604$ with 25 parameters. Positions and isotropic thermal parameters for all atoms included in the model may be found in Table IV while anisotropic thermal parameters and observed and calculated structure factors are tabulated in the supplementary material. Refinement of the model in the space group $P\bar{6}2c$ gave $R = 0.0600$ and $R_w = 0.0536$ with 36 least-squares parameters. Refinement of the model in the space group $P6_3mc$ gave $R = 0.0499$ and $R_w = 0.0633$ with 42 least-squares parameters. The Hamilton test was not used since both refinements in noncentrosymmetric space groups are severely underdetermined; hence, the centrosymmetric group was chosen for final refinement. The largest peak on the final electron-density difference map was found near the Cu ion position with a magnitude of 0.453 e/Å³.

## Results

**Low-Temperature Phase.** The crystal structure determination of Weenk and Spek[7] is confirmed as far as the $CuCl_3$ backbone is concerned. The unit cell of this phase is 5 times as large as the one of $CsNiCl_3$ (2L). The symmetry of this phase is rigorously reduced with respect to the parent structure. The main sources of deformation are the Jahn–Teller effect of the $CuCl_6$ octahedra and the size and orientation of the very large tetramethylammonium cations. The elongation of the octahedra resulting from the Jahn–Teller effect is larger than the one found in the related compound $\beta$-$CsCuCl_3$ (TMCuC, long axis 3.0 Å, short axis 2.3 Å; $\beta$-$CsCuCl_3$, long axis 2.8 Å, short axis 2.3 Å). A striking feature of this structure is the fact that it seems to be built up from two structural units that resemble $\beta$-$RbCuCl_3$ (two octahedra) and $\beta$-$CsCuCl_3$ (three octahedra). In the former Cu ions lie (nearly) on the chain axis, whereas in the latter the Cu ions show a helical displacement pattern with respect to this axis. Even the Jahn–Teller elongations and octahedron heights are comparable to those found in the Rb and Cs compounds. Furthermore, the nonlibrating TMA groups are situated within the $CsCuCl_3$-like block and the librating ones in the $RbCuCl_3$-like unit. Relevant bond distances and angles in the structure may be found in Table V. In Figure 4 a view of the chain and the TMA ions is depicted.

**Table VI.** Bond Lengths (Å) and Angles (deg) for Cu and Cl in the TMCuC Intermediate-Temperature Phase

| | | | |
|---|---|---|---|
| Cu(1)–Cl(1) | 2.289 (3) | Cu(2)–Cl(1) | 2.755 (4) |
| Cu(1)–Cl(2a) | 2.340 (6) | Cu(2)–Cl(2a) | 2.360 (6) |
| Cu(1)–Cl(3a) | 2.308 (8) | Cu(2)–Cl(3a) | 2.423 (8) |
| Cu(1)–Cl(2) | 2.873 (5) | Cu(2)–Cl(2) | 2.353 (5) |
| Cu(1)–Cl(3) | 2.816 (6) | Cu(2)–Cl(3) | 2.336 (6) |
| Cl(1)–Cu(1)–Cl(2a) | 86.4 (1) | Cl(2)–Cu(2)–Cl(3a) | 87.6 (2) |
| Cl(1)–Cu(1)–Cl(3a) | 87.5 (2) | Cl(1)–Cu(2)–Cl(3) | 85.2 (1) |
| Cl(1)–Cu(1)–Cl(2) | 84.7 (1) | Cl(2a)–Cu(2)–Cl(3) | 87.1 (2) |
| Cl(2)–Cu(1)–Cl(3a) | 78.4 (2) | Cu(1)–Cl(1)–Cu(2) | 78.8 (1) |
| Cl(1)–Cu(1)–Cl(3) | 84.7 (1) | Cu(1)–Cl(2a)–Cu(2) | 86.5 (2) |
| Cl(2a)–Cu(1)–Cl(3) | 77.1 (2) | Cu(1)–Cl(3a)–Cu(2) | 85.8 (3) |
| Cl(1)–Cu(2)–Cl(2a) | 76.2 (1) | Cu(1)–Cl(2)–Cu(2) | 75.4 (1) |
| Cl(1)–Cu(2)–Cl(3a) | 75.5 (2) | Cu(1)–Cl(3)–Cu(2) | 76.8 (2) |
| Cl(1)–Cu(2)–Cl(2) | 86.3 (1) | | |

**Table VII.** Bond Lengths (Å) and Angles (deg) for C and N in the TMCuC Intermediate-Temperature Phase

| | | | |
|---|---|---|---|
| C(1)–N | 1.45 (4) | C(1a)–N | 1.42 (2) |
| C(2)–N | 1.45 (3) | C(2a)–N | 1.44 (2) |
| C(3)–N | 1.41 (2) | C(3a)–N | 1.44 (4) |
| C(4)–N | 1.44 (2) | C(4a)–N | 1.43 (3) |
| C(1)–N–C(2) | 108 (2) | C(1a)–N–C(2a) | 110 (3) |
| C(1)–N–C(3) | 110 (3) | C(1a)–N–C(3a) | 110 (3) |
| C(2)–N–C(3) | 110 (2) | C(2a)–N–C(3a) | 109 (2) |
| C(1)–N–C(4) | 109 (2) | C(1a)–N–C(4a) | 110 (2) |
| C(2)–N–C(4) | 109 (2) | C(2a)–N–C(4a) | 110 (2) |
| C(3)–N–C(4) | 111 (3) | C(3a)–N–C(4a) | 109 (2) |

**Intermediate-Temperature Phase.** The copper ions in this phase lie at inversion centers, consistent with the often found local tetragonal symmetry about the copper ions. The structure consists of parallel chains of face-sharing elongated octahedra with three chlorine atoms forming bridging bonds between neighboring copper atoms and tetramethylammonium ions separating the chains. The chains run parallel to the $z$ axis. Two of the chlorine atoms, Cl(2) and Cl(3), are disordered about $z = 0.25$ with one site occupied 54.0 (4)% of the time. The other chlorine atom, Cl(1), is not disordered and forms a long bond (2.755 (4) Å) with Cu(2) and a short bond (2.289 (3) Å) with Cu(1). The disorder in the chlorine positions does not affect the geometry about Cu(2) since the bond distances between Cu(2) and the four disordered chlorine positions range from 2.341 to 2.406 Å, and thus the direction of the Jahn–Teller axis on Cu(2) remains invariant. The Cu(1)–Cl(2) and Cu(1)–Cl(3) bond distances, 2.873 (5) and 2.816 (6) Å, respectively, indicate disorder of the Jahn–Teller axis about Cu(1), the bond distances to the other chlorine atoms ranging from 2.289 to 2.331 Å. This disorder causes Cu(1) to have, on the average, a tetragonally compressed octahedral geometry. The $z$ projection of the Jahn–Teller axis on Cu(1), then, is located at ±60° from the $z$ projection of the Jahn–Teller axis on the neighboring Cu(2) atom. The $CuCl_6$ elongated octahedron is distorted (stretched) along the $z$ direction as indicated by internal Cl–Cu–Cl angles ranging from 75.4 to 87.7°. The Cu–Cl–Cu angle ranges from 85.6 to 86.8° for the symmetric bridge and from 75.2 to 78.8° for the asymmetric bridge. Bond lengths and angles between copper and chlorine atoms may be found in Table VI, and a view of the $CuCl_3$ chain is shown in Figure 5. Bond lengths and angles between nitrogen and carbon atoms are found in Table VII.

**High-Temperature Phase.** The copper atoms are situated at positions of $\bar{3}m$ symmetry while the chlorine atoms are on or disordered about the mirror plane at $z = 0.25$. As in the lower temperature phase, the structure consists of parallel chains of face-sharing $CuCl_6$ elongated octahedra. Now, because of the hexagonal symmetry, all three bridging chlorine atoms must be crystallographically equivalent. The resulting disorder of the Jahn–Teller elongation over the three "4-fold" axes imposes a disorder over three sites for the chloride ion. Two of the chloride ion positions are related by the mirror plane at $z = 0.25$; thus,

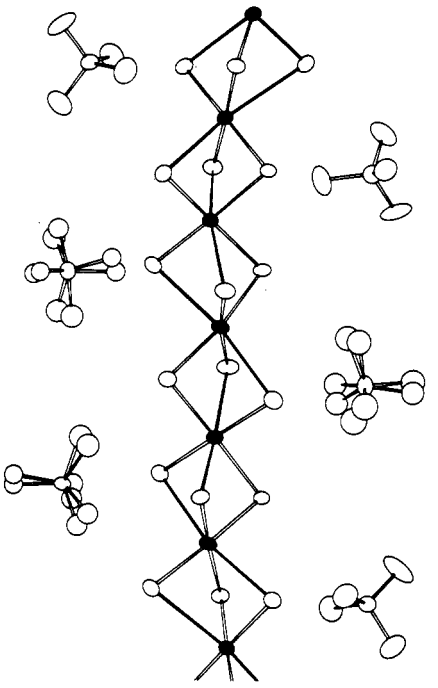

**Figure 4.** View of the low-temperature unit cell of TMCuC perpendicular to the *b* axis. Clearly visible are the two differently behaving TMA cations.

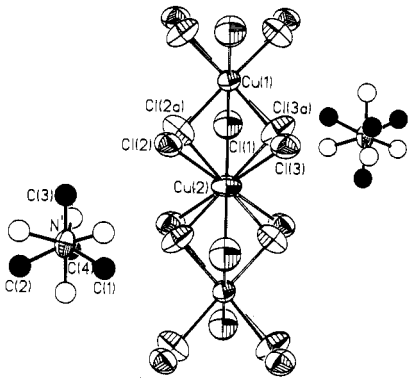


**Figure 5.** View of the $CuCl_3$ (323 K) chain and TMA ion perpendicular to the chain axis. Short bonds are open while darkened bonds represent the Jahn–Teller-elongated bonds. Darkened carbon atoms belong to the TMA ion orientation with 54 (2)% occupancy.

they must have the same fractional occupancy. One of these positions arises from the Jahn–Teller elongation of the octahedral axis. Since this elongated axis is disordered (by symmetry) over two other positions, the occupancy of this site must be $^1/_3$, as is the occupancy of the mirror-related site. The third ion position lies on the mirror plane at $z = 0.25$. Simple arithmetic then shows that the fractional occupancy of this chloride ion position is also $^1/_3$ (ignoring site symmetry). This scheme is the same as that reported by Crama[13] for the high-temperature hexagonal phase of $CsCuCl_3$. The chlorine ion position at $z = 0.25$ forms short bonds (2.29 (1) Å) with both copper atoms, while the positions off the mirror plane form a short bond (2.39 (1) Å) with one copper and a long bond (2.86 (1) Å) with the other copper atom. Since the chlorine atom forming a long bond with one copper ion forms a short bond with the adjacent copper ion in the chain, it is impossible for the *z* projection of the Jahn–Teller distortion axes of two neighboring copper atoms to have the same orientation. The $CuCl_6$ elongated octahedron is distorted (stretched) along the *z* direction, all internal Cl–Cu–Cl angles being less than 90°. Pertinent bond lengths and angles for the copper and chlorine

**Table VIII.** Bond Lengths (Å) and Angles (deg) for Cu and Cl in the TMCuC High-Temperature Phase[a]

| | | | |
|---|---|---|---|
| Cu–Cl | 2.29 (1) | Cu–Cl(1a) | 2.389 (9) |
| Cu–Cl(1) | 2.86 (1) | | |
| Cl–Cu(1)–Cl(b) | 75.6 (5) | Cl(1)–Cu(1)–Cl(1c) | 86.8 (2) |
| Cl–Cu(1)–Cl(1b) | 76.0 (3) | Cu–Cl–Cu(a) | 90.0 (6) |
| Cl–Cu(1)–Cl(1c) | 86.4 (4) | Cu–Cl(1)–Cu(a) | 75.5 (2) |

[a] Symmetry code: (a) $x, y, ^1/_2 - z$; (b) $-x, x - y, z$; (c) $-x, x - y, ^1/_2 - z$.

**Table IX.** Bond Lengths (Å) and Angles (deg) for C and N in the TMCuC High-Temperature Phase

| | | | |
|---|---|---|---|
| C(1)–N | 1.51 (3) | C(3)–N | 1.57 (3) |
| C(2)–N | 1.48 (4) | C(3a)–N | 1.56 (3) |
| C(1)–N–C(2) | 114 (1) | C(1)–N–C(3a) | 105 (1) |
| C(1)–N–C(3) | 105 (1) | C(2)–N–C(3a) | 109 (1) |
| C(2)–N–C(3) | 109 (1) | C(3)–N–C(3a) | 116 (2) |

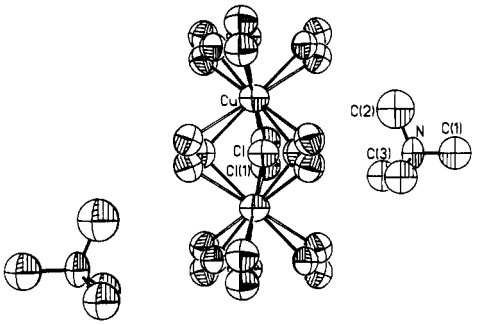


**Figure 6.** View of the $CuCl_3$ chain (405 K) including disorder of the chloride ion. Darkened bonds represent Jahn–Teller-elongated bonds, while open bonds represent short bonds. The chlorine atoms placed symmetrically between adjacent copper atoms have short bonds to both copper atoms.

atoms are listed in Table VIII. A view of the chain is shown in Figure 6. The nitrogen atom lies at a position with $\bar{6}m2$ symmetry, causing the tetramethylammonium ion to be disordered over six different orientations. Bond lengths and angles for the tetramethylammonium ion are listed in Table IX.

## Discussion

The high-temperature-phase structure corresponds closely to the structure determination by Crama for the high-temperature phase of $CsCuCl_3$. Refinement of the model with a single chloride ion position (on the mirror plane at $z = 0.25$) resulted in anisotropic chlorine thermal parameters in which $U_{33}$ was about twice $U_{11}$ and $U_{22}$. In addition the resulting electron density difference map showed a peak with height 0.79 e/Å$^3$, 0.486 Å from the chloride ion position. This was taken as evidence of disorder of the chloride ion about the mirror plane. Subsequent refinement of the disorder showed the disordered chlorine atoms to have nearly isotropic thermal parameters, $U_{ii}$ ranging from 0.06 to 0.09 Å$^2$. We conclude that the Jahn–Teller distortion is disordered in a manner that is isostructural with that of the $\alpha$ phase of $CsCuCl_3$ and in support of Crama's thesis.

A phase isostructural with the intermediate-temperature phase has not been observed in any $ACuCl_3$ system to date. $\beta$-$RbCrCl_3$, an analogous compound, shows the same intrachain elongation sequence.[14] When the three octahedral 4-fold axes are designated by *x*, *y*, and *z*, the Jahn–Teller elongation sequence along the hexagonal axis can be denoted by (*z*), (*x* or *y*), (*z*), (*x* or *y*), etc. From the crystallographic data it cannot be determined whether the Jahn–Teller effect is disordered on the Cu site, e.g., switching from *x* to *y*, or whether the elongation direction is static at a particular site but has different orientations at equivalent positions in the crystal. This elongation sequence along the hexagonal axis has been explained by Crama and Maaskant[14] for $\beta$-$RbCrCl_3$,

(13) Crama, W. J. *Acta Crystallogr., Sect. B: Struct. Crystallogr. Cryst. Chem.* **1981**, *B37*, 2133.

(14) Crama, W. J.; Maaskant, W. J. A. *Physica B+C* **1983**, *121B*, 219.

using a theory developed by Höck et al.,[15] in terms of site entropy and $E_{1g}$ and $E_{2g}$ strain components. Variable-temperature EPR experiments are under way to try to identify the nature of the disorder.

The low-temperature phase can be characterized by stating that the disorder resulting from the entropy mentioned above (the energy gain of which decreases when the temperature is lowered) is overruled by energy gain that results from fixing the Jahn-Teller elongation at the bottom of the wells of the warped potential energy surface, the so-called Mexican hat. This mechanism also prevents incommensurability but does not explain the 5-fold unit cell.

Recently some authors[3] have tried to describe this kind of Jahn-Teller system with a pseudospin model as mentioned in the Introduction. Concerning the intermediate phase of both $RbCrCl_3$ and TMCuC, it is more difficult to imbed those in a pseudospin Ising system since this model does not allow for self-entropy of the Cu site. This fact makes it impossible to describe the successive transitions in TMCuC in the light of a "devil's staircase" as formulated by, e.g., Bak[16] for magnetic spins. Another model, the ANNNI model,[17] applied to $CsCuCl_3$ and the low-temperature TMCuC reveals that the ordering of the Jahn-Teller-elongated axes in the former compound is much more stable, by a factor of 5, than the one found in TMCuC. This model can therefore not explain this low-temperature structure. This in fact does not surprise us, as it is shown in a recent paper by Maaskant and Haije[18] that apart from the usual quadrupolar deformations, due to the Jahn-Teller effect, also dipolar distortions and their mutual interactions have to be taken into account. This would lead, in the case of TMCuC, to a complicated pseudospin-phonon coupling scheme. Furthermore, the low-temperature structure described in this paper is not the $T = 0$ K structure. Recent magnetic measurements on a single crystal of TMCuC revealed a phase transition at about 140 K. X-ray experiments showed the crystal to transform to a multidomain structure. Neutron diffraction experiments will be carried out in the near future to determine this crystal phase.

**Acknowledgment.** The support of NSF Grant CHE-8408407 and of The Boeing Co. in the establishment of the X-ray diffraction facility at Washington State University is gratefully acknowledged, as is the support of the donors of the Petroleum Research Fund, administered by the American Chemical Society. The investigations were supported in part (W.G.H.) by the Netherlands Foundation for Chemical Research (SON) with financial aid from the Netherlands Organization for the Advancement of Pure Research (ZWO). The Netherlands Organization for the Advancement of Pure Research is acknowledged for a visiting professorship for R.D.W.

**Registry No.** $(CH_3)_4NCuCl_3$, 58428-65-2.

**Supplementary Material Available:** Tables of anisotropic thermal parameters for $(CH_3)_4NCuCl_3$ at 213, 323, and 405 K and hydrogen atom coordinates for $(CH_3)_4NCuCl_3$ at 213 and 323 K (5 pages); tables of observed and calculated structure factors for $(CH_3)_4NCuCl_3$ at 213, 323, and 405 K (27 pages). Ordering information is given on any current masthead page.

(15) Höck, K.; Schröder, G.; Thomas, H. *Z. Phys. B: Condens. Matter Quanta* **1978**, *30*, 403.
(16) Bak, P. In *Recent Developments in Condensed Matter Physics*; De Vreese, J. T., Ed.; Plenum: New York, 1981; Vol. I, p 489.
(17) Fisher, M. E.; Selke, W. *Philos. Trans. R. Soc. London, A* **1981**, *302*, 1.
(18) Maaskant, W. J. A.; Haije, W. G. *J. Phys. C* **1986**, *19*, 5295.

Contribution from the Department of Physics, Clark University, Worcester, Massachusetts 01610, and Department of Chemistry, Washington State University, Pullman, Washington 99164

# Alternating Exchange in Homonuclear Ferrimagnetic Linear Chains. Tetrakis(tetramethylene sulfoxide)copper(II) Hexahalodicuprate(II) (Halo = Chloro, Bromo): Crystal Structures and Magnetic Susceptibilities

C. P. Landee,*† A. Djili,† D. F. Mudgett,† M. Newhall,† H. Place,‡ B. Scott,‡ and R. D. Willett*‡

*Received September 4, 1987*

The two compounds $\{Cu(TMSO)_4\}[Cu_2X_6]$ (X = Br (**1**) and Cl (**2**); TMSO = tetramethylene sulfoxide) have been synthesized and their crystal structures determined at room temperature. They are isostructural, and both crystallize in the triclinic system, space group $P\bar{1}$, with cell parameters for **1** of $a = 8.448$ (2) Å, $b = 9.630$ (2) Å, $c = 11.655$ (2) Å, $\alpha = 65.42$ (1)°, $\beta = 71.59$ (2)°, and $\gamma = 73.52$ (1)°. The cell parameters of **2** are $a = 8.250$ (4) Å, $\beta = 9.330$ (5) Å, $c = 11.131$ (6) Å, $\alpha = 67.59$ (4)°, $\beta = 73.29$ (6)°, and $\gamma = 74.67$ (6)°. The structures consist of alternating chains of dimeric $Cu_2X_6^{2-}$ anions and monomeric $Cu(TMSO)_4^{2+}$ cations extended along the $c$ axes. The magnetic properties have been investigated down to 1.4 K. Both compounds show evidence of two types of magnetic interactions: ferromagnetic exchange within the dimeric units ($J_d(Br)/k = 12$ (4) K, **1**; $J_d(Cl)/k = 20$ (5) K, **2**) and a weaker exchange between the dimeric and monomeric copper atoms that is antiferromagnetic for **1** ($J_m(Br)/k = -1.5$ K) and ferromagnetic for **2** ($J_m(Cl)/k = 1.6$ K). The magnetic susceptibility of the bromide salt, **1**, is interpreted in terms of a ferrimagnetic linear-chain model where the ferrimagnetism of the homometallic system arises from an odd number of magnetic atoms per unit cell. The corresponding chloride salt, **2**, represents a ferromagnetic chain, with no evidence of any antiferromagnetic interchain coupling observable down to the lowest temperature measured.

## Introduction

The discovery of ordered, bimetallic linear chains[1] has opened up new possibilities in magnetochemistry. These materials consist of two different transition-metal ions bridged by either carboxylate groups[2] or substituted oxalate groups[3-5] in a ...-M-L-M'-L-M-... pattern and thus permit the magnetic pairing of a wide variety of metal ions. The magnetic interactions have inevitably been found to be antiferromagnetic, but the anisotropy of the superexchange is controlled by the specific ions involved: the behavior of the $Co^{2+}$ ion is always best described by the anisotropic Ising model,[6] while $Mn^{2+}$, $Ni^{2+}$, and $Cu^{2+}$ systems have been modeled

* To whom correspondence should be addressed.
† Clark University.
‡ Washington State University.

(1) For a review, see: Landee, C. P. In *Organic and Inorganic Low Dimensional Crystalline Materials*; Drillon, M., Delhaes, P., Eds.; NATO ASI Series; Plenum: New York; in press.
(2) Beltran, D.; Escriva, E.; Drillon, M. *J. Chem. Soc., Faraday Trans. 2* **1982**, *78*, 1773.
(3) Gleizes, A.; Verdaguer, M. *J. Am. Chem. Soc.* **1984**, *106*, 3727.
(4) Verdaguer, M.; Julve, M.; Michalowicz, A.; Kahn, O. *Inorg. Chem.* **1983**, *22*, 2624.
(5) Pei, Y.; Verdaguer, M.; Kahn, O.; Sletten, J.; Renard, J.-P. *Inorg. Chem.* **1987**, *26*, 138.
(6) Georges, R.; Curély, J.; Drillon, M. *J. Appl. Phys.* **1985**, *58*, 914.

0020-1669/88/1327-0620$01.50/0 